CAPILLARY FLOW POROMETRY – ASSESSMENT OF AN ALTERNATIVE METHOD FOR THE DETERMINATION OF FLOW RELEVANT PARAMETERS OF POROUS ROCKS

Matthias Halisch[(1)], Esther Vogt[(1)], Cornelia Müller[(1)], Angels Cano-Odena[(2)], Danny Pattyn[(2)], Patrice Hellebaut[(2)], Kees van der Kamp[(2)]

[(1)]Leibniz Institute for Applied Geophysics (LIAG), Stilleweg 2, D-30655 Germany
[(2)]POROMETER N.V., Begoniastraat 17, 9810 Eke, Belgium

This paper was prepared for presentation at the International Symposium of the Society of Core Analysts held in Napa Valley, California, USA, 16-19 September, 2013

ABSTRACT

The determination of flow relevant parameters of porous rocks (e.g. permeability, pore throat radii distribution, pore size distribution, porosity, to name only few) forms since decades a well established part of petrophysics to characterize, understand and assess reservoir rocks in terms of their hydraulic properties and flow behavior. For the determination of the pore throat radii / pore size distribution of porous rocks, the mercury injection technique (after Purcell) is commonly used. With this technique, the rock sample is flooded with mercury, whereat the applied injection pressure is proportional to the size of the pores (pore throats), which are through-flown. Nevertheless, this technique is not only time consuming (several hours), the sample is strongly mechanically influenced, due to the high overburden / injection pressure (up to 10,000 psi) and additionally, it is contaminated with mercury. Contaminated rock samples are very difficult to handle, toxic and, in most cases, the valuable core sample is lost for further investigations. The authors would like to present a promising alternative to this well established method, the so called Capillary Flow Porometry (CFP). Originally developed for the characterization of filter papers, porous membranes and other nanostructure materials, this technique has been successfully adapted for petrophysical purposes by a first prototype. Contrary to Hg-injection, CFP uses an inert gas (e.g. nitrogen) to push a wetting and nontoxic liquid out of the porous network, where the applied pressure is again inversely proportional to the corresponding pore / pore throat. Furthermore, measuring time is greatly reduced from several hours to several minutes. First measurements on different cretaceous sandstones show good reproducibility and good accordance to Hg-injection experiments. Additional core and special core analyses (CAL / SCAL) have been carried out (permeability, BET surface, porosity, NMR, µ-CT), to characterize the corresponding porous networks as complete as possible, and to correlate results of the Hg-injection and CFP meaningful.

INTRODUCTION

CFP is currently applied in both academic and industrial organizations. Most of the applications of this technique are in new materials, products research and development as well as in quality control routine tests. CFP is a very versatile technique and it is used to characterize porous materials of different chemical nature and for different end-applications, e.g. in the textile and non-woven industry, it is widely used for pore size distribution measurements but also especially for bubble point tests and in quality control of non-woven materials and supports. Other common products that are characterized by CFP are filter media, ultra and microfiltration polymeric membranes [1] and hollow fibers [2] used in water treatment [3 & 4], medical or energy applications [5]. Battery electrodes, paper, cigarette filters, ceramic membrane modules and zeolites are other examples of applications. Nevertheless, it seems to be a feasible technique to be adapted for petrophysical investigations of natural rocks as well, since the main pore throat diameter range of interest of porous and permeable rocks, is investigated (figure 1).

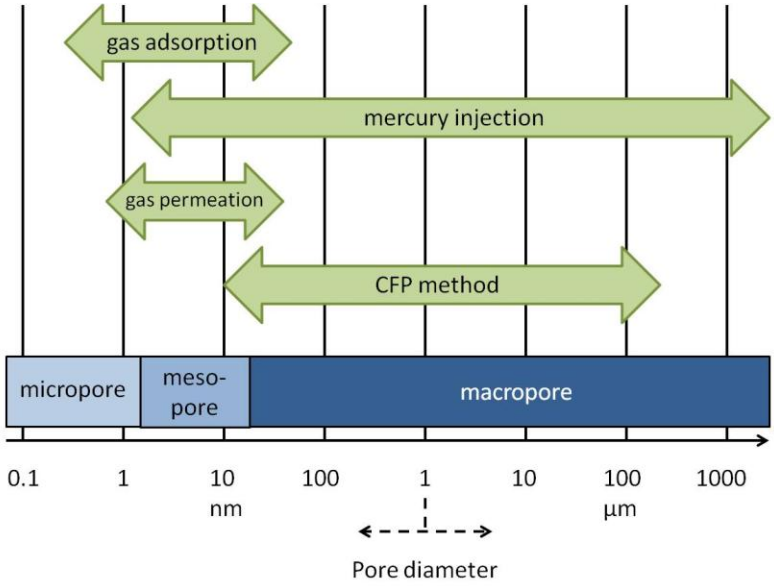

Figure 1: Typical measuring ranges for the determination of pore (throat) diameters by conventional methods (gas adsorption, Hg-injection, gas permeation) and by the Capillary Flow Porosimetry technique.

THEORY OF CFP

The pores present in materials can be classified in three main groups, depending on the pore path type. The first group corresponds to closed pores, the second group refers to blind pores, in which the pore path starts at one surface and terminates inside the material. The third group comprises the so-called through pores, which are interconnected through the entire material. Figure 2 illustrates these three different types. Closed and blind pores do not contribute to the flow through the material. Therefore only the connected pores are investigated by CFP, and obviously, these are the pores of interest and that need to be characterized for fluid transport within the rock matrix.

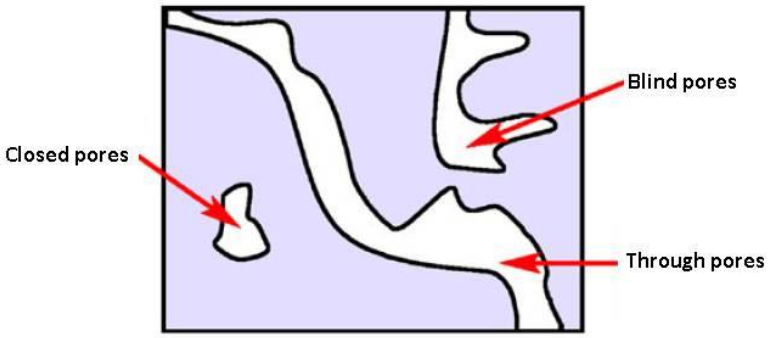

Figure 2: Different schematic pore types which can be found in a huge variety of materials including natural rocks.

Prior to a capillary flow porometry measurement it is necessary to impregnate the samples with a wetting liquid. An inert gas, normally N_2, is used to displace this wetting liquid from the porous network. The pressure required to empty a pore corresponds to the pressure necessary to evacuate the liquid from the most constricted part of it [1] (see figure 2). This most constricted part is the most challenging one and it offers the highest resistance to remove the wetting liquid. The Young-Laplace formula permits calculating the pore diameter from the measured pressure:

$$P = 4*\gamma*\cos\theta/D \qquad (1)$$

Where D is the pore size diameter, P is the measured pressure, γ is the surface tension of the wetting liquid and θ is the contact angle of the wetting liquid with the sample [6]. The surface tension γ depends on the wetting liquid used. The contact angle θ depends on the interaction between the material and the wetting liquid. The different wetting liquids used in CFP enter spontaneously the porous sample network and ensure a complete wetting of the material. Therefore the contact angle of the wetting liquid with the sample equals zero and the previous formula can be expressed simplified as:

$$P = 4*\gamma/D \qquad (2)$$

The selection of the wetting liquid determines the measureable pore size range for a given pressure. Water, alcohols, silicone oil and perfluoroethers are common wetting liquids used in CFP. Water and/or alcohols can easily evaporate and the samples may partially dry before the actual porometry test begins. Moreover water, for instance, has a relatively high surface tension (γ = 72 dynes/cm) compared to perfluoroethers (e.g. γ = 16 dynes/cm). This means that in order to measure the same pore size using water as a wetting liquid it is necessary to apply a pressure more than 4 times the pressure required, if perfluoroethers are used, so that these liquids are preferred by the CFP (here: γ = 18 dynes/cm) . They have very low surface tension and low vapor pressure (i.e. do not easily evaporate) and, in general, they do not react with samples neither cause their swelling. In principle there is no universal wetting liquid and the choice of one or another depends on

the application and the type of sample to be characterized. Nevertheless, it is important to use the same wetting liquid when comparing results.

There are two measurement methods for CFP and the selection of the best one depends on the type of application and purpose of the test. The pressure scan method is the traditional approach (figure 3, left hand side). The pressure increases continuously at a constant rate and the gas flow through the sample is measured. The rate of pressure increase and the number of data points recorded during the measurement can be adjusted by the user.

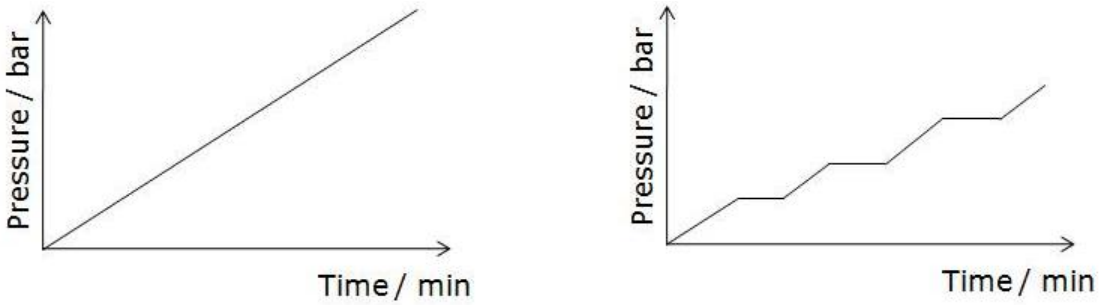

Figure 3: Continuous increase of pressure in time (left hand side) and increase of the pressure with respect of time in steps, holding the actual pressure for a certain time before increasing it to the next value (right hand side).

This method is fast, very reproducible and it is recommended for quality control. When the materials present a complex structure with pores of different shapes and tortuosity it can lead to some inaccuracy in the pore size determination. During the pressure scan pores with the same diameter but longer pore path may not be emptied at the pressure corresponding to their diameter (if the scan is too fast there is not enough time to allow the gas flow to displace the wetting liquid through the pore length). Therefore the longer pores will be detected at higher pressures (later in time) and report smaller diameters than they actually possess.

A more accurate measurement of the pore sizes is possible with the so-called pressure/step stability method [2]. In this case a data point is only recorded when the pressure is held at a constant value for a user-defined time (figure 3, right hand side) and also the flow of gas through the sample meets the stability criteria defined by the user. This allows enough time for the gas flow to displace the wetting liquid in pores of the same diameter with different length and tortuosity. This is confirmed by measuring a stable gas flow before increasing the pressure to the next value. Because it takes the different tortuosity and length of pores with the same diameter into account, this method is the most recommended one for research and development of applications. It is the one that has been used in the present work. Additionally, the pressure step/stability measuring principle allows measuring the true First Bubble Point, which is associated to the maximum pore size (entry pressure of the largest pore) [7].

PROCEDURE

One of the advantages of CFP over other pore characterization techniques is that it permits obtaining several parameters and information with good accuracy and reproducibility in one individual and fast measurement. Normally the measurement with the dry sample (“dry run”) is carried out first. Afterwards the wet sample (impregnated with wetting liquid) or "wet run" is performed. The "wet curve" is the representation of the measured gas flow against the applied pressure. The half-dry curve is obtained by dividing the flow values of the dry curve by 2 and it is also plotted against the applied pressure in the same graphic. From the representation of these three curves it is possible to identify information about porous network of the sample. The maximum pore size (FBP) is determined as soon as gas flow through the sample is detected. The mean flow pore size corresponds to the pore size calculated at the pressure where the wet curve and the half-dry curve meet. It corresponds at the pore size at which 50 % of the total gas flow can be accounted. The minimum pore size is calculated at the pressure at which the wet and the dry curve meet (from this point onwards the flow will be the same because all the pores have been emptied). Figure 4 shows a scheme of the three curves and parameters measured in CFP.

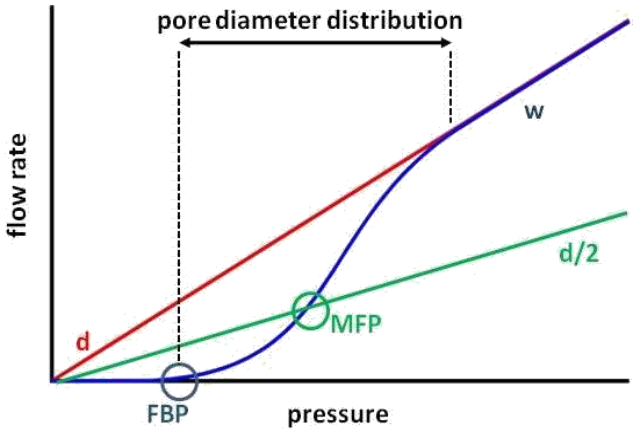

Figure 4: Exemplary measuring curves and resulting parameters in CFP (d = dry curve, w = wet curve, d/2 = half-dry curve, FBP = largest pore, MFP = mean flow pore).

Apart from this information, it is possible to obtain the cumulative filter flow distribution against the pore size from the same CFP measurement. It provides information of the percentage of the cumulative total flow through the sample. Furthermore, the corrected differential filter flow can be additionally plotted, which shows the flow distribution per unit of change in size - i.e. the increase in flow rate per unit increase in pore diameter, which is most commonly defined as pore size distribution.

THE POROLUX 1000 DEVICE

All the CFP measurements in this work were carried out by using a POROLUX™ 1000 porometer (figure 5, right hand side), designed and supplied by POROMETER N.V. (Belgium). The POROLUX™ 1000 uses the pressure step/stability method as described in the previous section. The combination of a very accurate entry pressure regulator and a specially designed needle valve controls both the pressure increase and the pressure in the

most precise way, resulting in a very accurate measurement of the pore size. A data point is only recorded when the stability algorithms (defined by the user) are met for both pressure and flow. This means that the porometer solely detects when a pore empties at a certain pressure and waits until all pores of the same diameter have been completely emptied before accepting a data point. The FBP is measured when a deviation of the linear pressure increase (or the first derivative) over time is detected (figure 5, left hand side), which means that the largest pore is open and the gas flow is going through the sample.

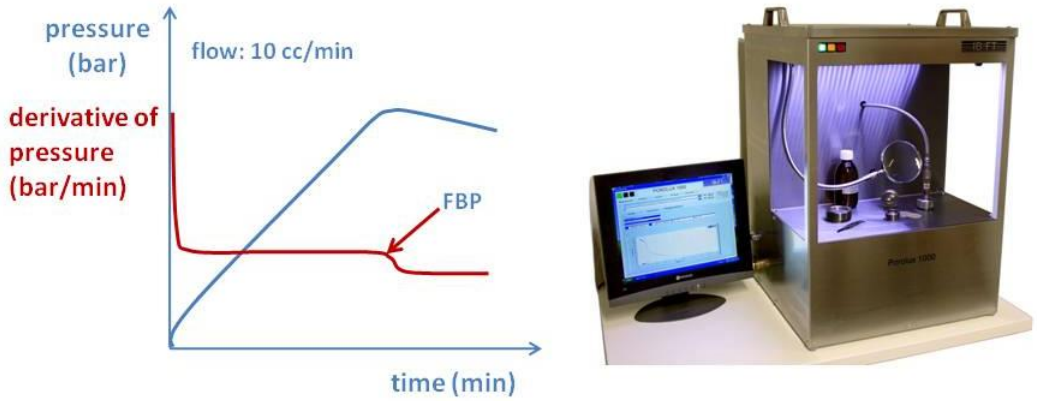

Figure 5: Linear pressure increase and the first derivative of pressure as a function of time in a first bubble point measurement (left hand side) and the POROLUX 1000 device (right hand side).

Product overview	POROLUX™ 1000	POROLUX™ 1000LP	POROLUX™ 1000LF
Max pressure	3.5 MPa/500 psi	0.8 MPa/116 psi	3.5 MPa/500 psi
Min pore	13 nm	80 nm	13nm
Max pore	500 µm	500 µm	500 µm
Max flow	200 l/min	100 l/min	10 l/min
Sample holders	13-25-47 mm	25 mm	13-25-47 mm
Pressure sensors	5-50 bar	1-10 bar	5-50 bar
Flow sensors	10-200 l/min	5-100 l/min	0,5-10 l/min

Table 1: Overview of the POROLUX product series, including the main measuring features of each device. The POROLUX 1000 (column 2) has been used for this assessment.

SAMPLE DESCRIPTION & PREPARATION

For the assessment of the CFP technique, different types of cretaceous sandstones have been used. For this paper, the results of one exemplary sandstone are shown. This sandstone is known as “Bentheimer sandstone”, which is comparable to the also well known Berea and Fontainebleau type sandstones. This rock is mineralogically characterized as quartz sandstone with about 10-14% feldspar and up to 6% clay content. Overall, it is well sorted and classified [8]. Predominating matrix grain size has been determined to be in range of 250 - 450 microns. The features influencing the pore structure are identified to be weathered feldspars as well as illite booklets (figure 6). Small amounts of clay minerals are always located in the vicinity of partial dissolved feldspar minerals. These accumulations appear in two different ways: first, as (partial) coatings around quartz grains, second, as fillings of interparticle porosity. Additionally, this sandstone has been extensively investigated by a large variety of CAL and SCAL experiments [9]. CAL experiments have been conducted on a total of 50 core plug samples (40mm length, 30mm diameter each) to ensure a good statistical parameter spreading. For SCAL experiments (e.g. the Hg-injection), smaller subsample sets, consisting of 5 plug samples, have been formed.

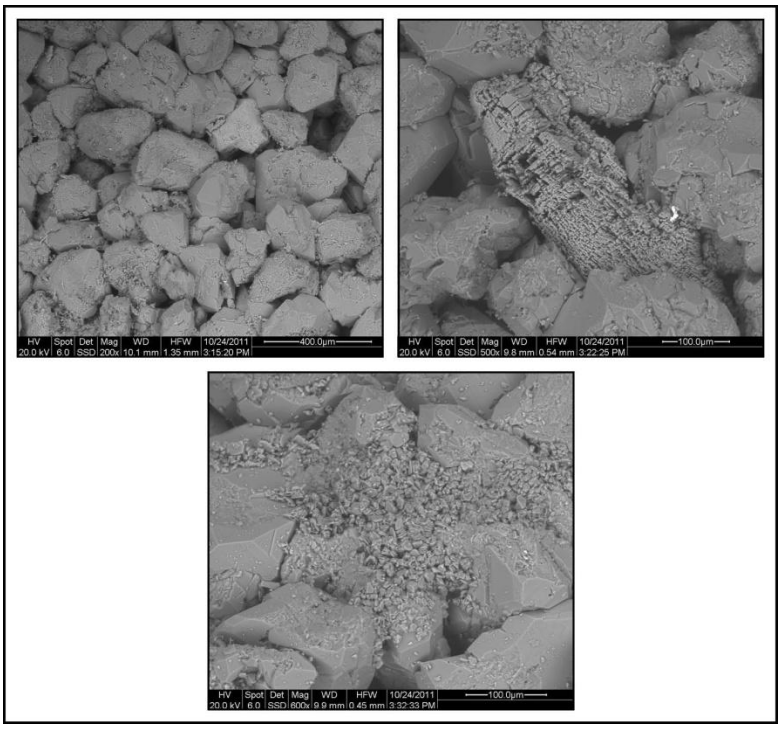

Figure 6: Exemplary Scanning Electron Microscopy (SEM) images of the Bentheimer sandstone specimen. Upper left side: overview on the matrix; upper right side: dissolved feldspar; bottom: illite booklets. [9]

The results of the petrophysical investigations are conclusive with the mineralogical description. Nevertheless, main focus of the research was upon the characterization of the pore space. The Bentheimer sandstone exhibits good porosity (average of 21.5%) and good permeability (average 593 mD), and the specific surface area is within the expected

dimension (average 0.45 m^2/g), which is consistent with the small amount of clay (figure 7). These findings point to a good and interconnected porous network, consisting of mainly “large”, i.e. macropores, and few meso- to micropores due to the pore structures added by dissolved mineral phases and clay, respectively.

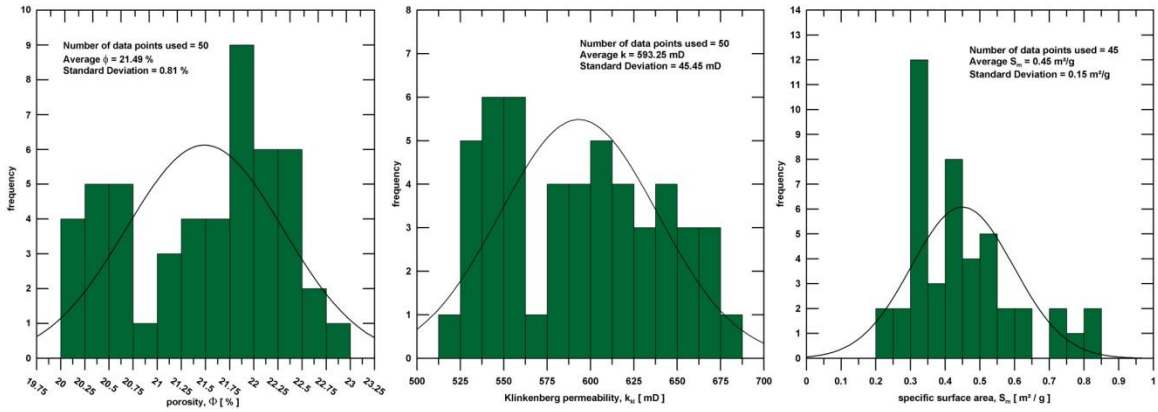

Figure 7: Porosity, Klinkenberg gas permeability and specific surface distribution for the Bentheimer sandstone sample set [9].

Figure 8 allegorizes this assumption by the averaged results of NMR relaxation time spectra and – additionally and for example – by a conventional Hg-injection experiment. As shown, NMR experiments (figure 8, right hand side) indicate mostly free movable pore water (cut off time > 33ms), which directly correlates with large pores (91 %). About 7.5 % correlate to capillary water, whereas 1.5 % can be linked to clay bound water. Hg-injection experiments confirm these findings (figure 8, left hand side). Predominating pore throat size is about 15 µm, which can be linked to the throats formed by the quartz matrix. Due to scanning electron microscopy investigations (figure 6) and micro-CT imaging (figure 9), throat sizes smaller than 5 µm correlate with pore networks, formed by dissolved mineral phases, whereas throats smaller than 500 nm can be attached to the local pore networks between the clay booklets as well as between the clay minerals (throats < 0.04 µm). Summarized, the pore network of the Bentheimer sandstone has been studied most completely to understand the complex relationships, which influence and form the observed structures. These combined findings form a good fundament for the application of the CFP technique and of the results therefrom.

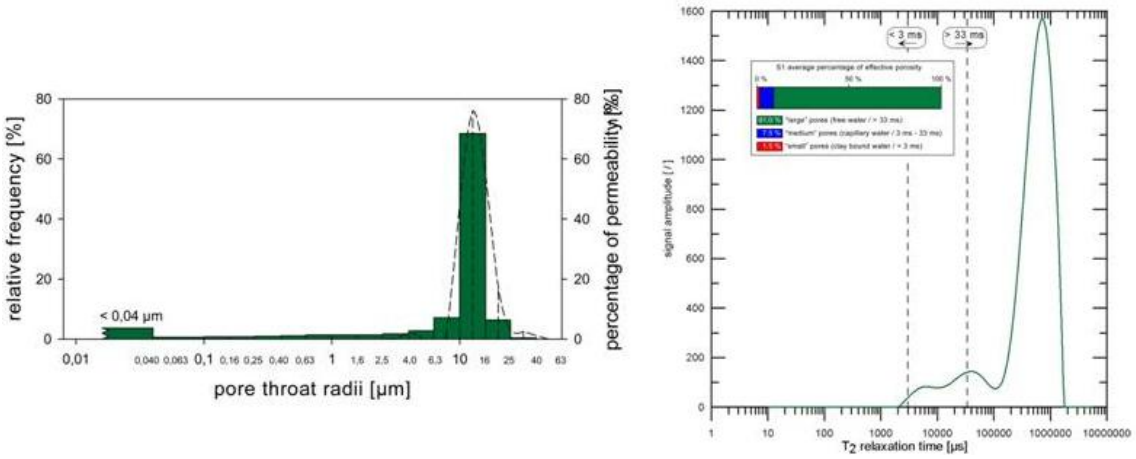

Figure 8: Exemplary pore throat radii distribution derived by Hg-injection for the sample used in this study (left hand side), and averaged T_2 relaxation time spectrum and average percentage of effective porosity for the entire Bentheimer sandstone specimen set (right hand side) [9].

Since the standard size porometer cell is smaller than the regular plug size, a slice of 4-5 mm needed to be cut from the end of the plug. The sandstone slice has been used for the CFP measurement, whereas the rest of the plug has been used for the conventional Hg-injection. By this, a direct comparison of results can take place. Before the measurement the sample has been dried to ensure, that no fluid is inside the void space. After the drying process, the specimen has been placed inside the sample cell and the "dry curve" has been measured. Following, the sample has been saturated with a special wetting fluid as described within the theory section of this paper. Micro-CT imaging has shown, that the pore space has been saturated almost completely (98 %, figure 9, right hand side), just by placing the sample inside a vessel filled with the wetting liquid.

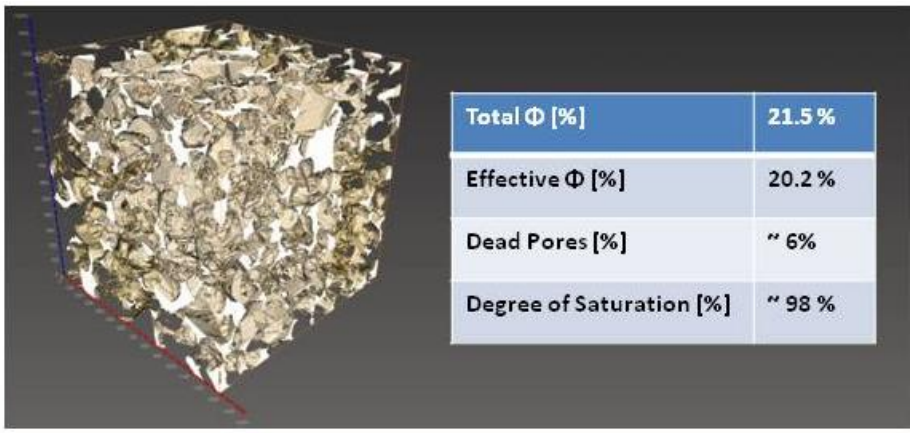

Figure 9: Micro-CT image of the pore network of the Bentheimer sandstone specimen (left hand side) and pore space parameters derived by quantitative image analysis (right hand side).

RESULTS

In total, six repeated measurements have been performed to evaluate the reproducibility of the CFP technique (figure 10). As shown, this method offers good reproducibility, even after several wetting-drying-wetting cycles. Additionally, measurements obey high resolution, since each curve consists of about 200 measuring points. Remarkably, each measuring cycle (wetting-drying) took only about one hour, so that in total, this experiment has been performed in less than seven hours. This cycle experiment equals almost the time of *one* conventional Hg-injection experiment within the same measuring range. Next, the curves have been processed (average of cycle 2-6, deleting cycle 1 due to sample holder leakage as well as deleting all values > 50 µm, due to pressure inducer instability) and binned (figure 11, left hand side), which clearly shows the higher accuracy within the pore throat distribution, than it is achieved for mercury experiments. To compare the results directly with the conventional pore radii distribution – in terms of pore throat bin – a polynomial fitting (best fit: sixth order polynom; residual sum of squares: 7.45; R-squared: 0.962) needs to be applied, in order to recalculate the area underneath the fitting curve to the same bin sizes that have been used for the mercury experiment (figure 11, right hand side).

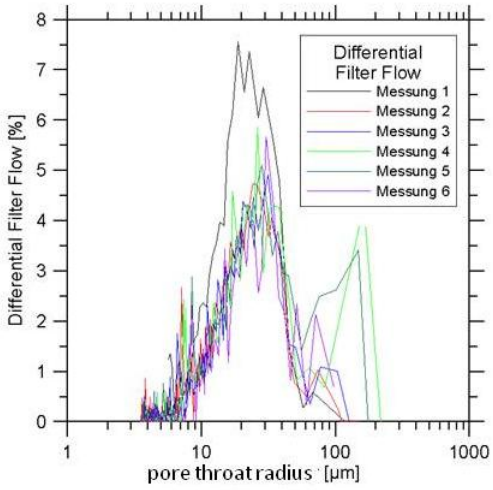

Figure 10: Resulting pore throat radii distributions for six measuring cycles (wetting-drying-wetting) on the Bentheimer specimen. The results indicate high resolution combined with good reproducibility.

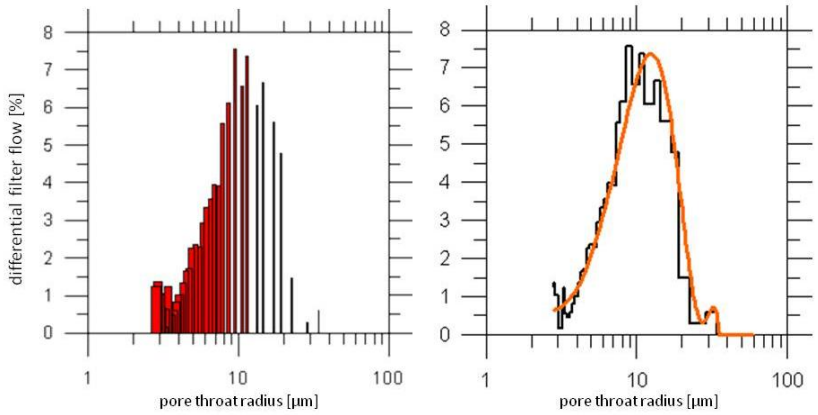

Figure 11: Averaged and recalculated pore throat distribution (left hand side) and polynomial fitting for better comparison with results of the conventional mercury injection experiment (right hand side).

For comparison, the resulting pore throat bins have been plotted within the pore throat radii distribution as shown within figure 8. Figure 12 allegorizes the results of both techniques, showing good accordance with each other! Obviously, results of the CFP measurements "scatter" a little bit more on the flanks of the main pore throat size. This is an effect of the recalculation for the comparison of both measurements, since the original CFP data do have smaller bins, which equals higher resolution.

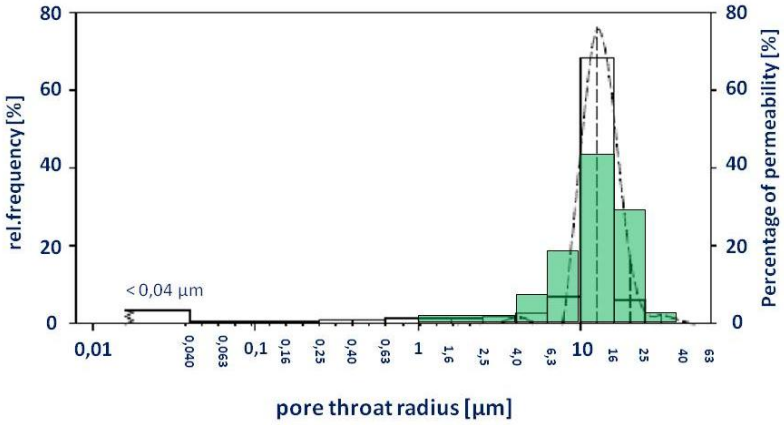

Figure 12: Comparison between the pore throat radii distribution, that has been derived by Hg-injection (faded out) and by the CFP technique (light green). Both measuring techniques indicate good accordance.

CONCLUSIONS

This very first application of the CFP technique for the determination of pore throat radii distributions of porous rocks has delivered remarkably good results. Additionally, they are in good accordance with conventional mercury injection experiments. Despite of this, the CFP technique is significantly faster and shows a good reproducibility. The measuring time has been reduced to 1 hour per cycle, including preservation of the sample for further investigations. Although the repeated measuring cycles do scatter, overall accuracy was good, in accordance to the Hg-injection experiments. It is expected, that these scattering effects got reduced, by adapting and developing the sample holder for this specific need. Due to the non toxic wetting fluid in combination with the significantly smaller pressures that need to be applied, the valuable specimen can be used for further investigations and laboratory experiments. For porous and permeable sandstones (e.g. the Bentheimer / Berea / Fontainebleau type), this technique seems to be a versatile and feasible alternative for the determination of the (hydraulic effective) pore throat radii distribution.

OUTLOOK

In the near future a larger cell is planned to increase the representativeness of the CFP measurements, i.e. to increase sample size to lab scale. Besides, a new leakage cover will be implemented, to increase cycle stability. Additionally, it is planned to measure pressure dependent gas, as well as liquid permeability by installing small liquid reservoir onto the POROLUX device. Furthermore, the software is going to be adapted, to optimize the measuring procedure (e.g. equidistant pressure steps) and evaluation

routines. A routine workflow is under development, to increase the overall data quality, especially for the sample preparation before and in between the cyclic measurements. Next, different and more complex types of sandstone as well as carbonate rocks are going to be investigated, to assess the CFP technique on a broader range of rock types.

REFERENCES

1. Agarwal, C.; Pandey, A. K.; Das, S.; Sharma, M. K.; Pattyn, D.; Ares, P.; Goswami A. Neck-size distributions of through-pores in polymer membranes. *Journal of Membrane Science*, 2012, Vol. 415–416, 608–615.

2. Francis, L.; Maab, H.; AlSaadi, A.; Nunes, S.; Ghaffour, N.; Amy, G.L. Fabrication of electrospun nanofibrous membranes for membrane distillation application *Desalination and Water Treatment*, 2013 Volume 51, Issue 7-9, pages 1337-1343.

3. Low, S.C.; Ahmad, A.L.; Ideris, N.; Ng, Q.H. Interaction of isothermal phase inversion and membrane formulation for pathogens detection in water *Bioresource Technology*, Volume 113, June 2012, Pages 219-224.

4. Ahmad, A. L.; Ideris, N.; Ooi, B. S.; Low, S. C.; Ismail, A. Synthesis of polyvinylidene fluoride (PVDF) membranes for protein binding: Effect of casting thickness *Journal of Applied Polymer Science* 2013, Volume 128, Issue 5, pages 3438–3445.

5. Maab, H.; Francis, L.;, AlSaadi, A.; Aubru, C.; Ghaffour, N.; Amy, G.L.; Nunes, S. P. Synthesis and fabrication of nanostructured hydrophobic polyazole membranes for low-energy water recovery. *Journal of Membrane Science* 2012, Volume 423-424, Pages 11-19.

6. S. Lowell; J. E. S. Martin; A. Thomas; M. Thommes. *Characterization of Porous Solids and Powders: Surface Area, Pore Size and Density*; Springer: Dordrecht, 2006.

7. ASTM F-316-03: "Standard Test Methods for Pore Size Characteristics of Membrane Filters by Bubble Point and Mean Flow Pore Test".

8. Stadtler, A. Der Bentheimer Sandstein (Valangin, NW-Deutschland) : eine palökologische und sequenzstratigraphische Analyse. *Number 49 in Bochumer geologische und geotechnische Arbeiten 1998. Ruhr-Universität Bochum : Inst. für Geologie 1998.*

9. Halisch, M. Application and Assessment of the Lattice Boltzmann Method for Fluid Flow Modeling in Porous Rocks. *PhD Thesis.* (http://nbn-resolving.de/urn:nbn:de:kobv:83-opus-39381). Technische Universität Berlin, 2013, Berlin, Germany.